

Interdependence of Endomembrane Trafficking and Actin Dynamics during Polarized Growth of Arabidopsis Pollen Tubes^{1[C][W][OA]}

Yan Zhang², Junmin He², David Lee, and Sheila McCormick*

Plant Gene Expression Center, United States Department of Agriculture/Agricultural Research Service, and Department of Plant and Microbial Biology, University of California at Berkeley, Albany, California 94710 (Y.Z., J.H., D.L., S.M.); and School of Life Sciences, Shaanxi Normal University, Xi'an 710062, People's Republic of China (J.H.)

During polarized growth of pollen tubes, endomembrane trafficking and actin polymerization are two critical processes that establish membrane/wall homeostasis and maintain growth polarity. Fine-tuned interactions between these two processes are therefore necessary but poorly understood. To better understand such cross talk in the model plant *Arabidopsis thaliana*, we first established optimized concentrations of drugs that interfere with either endomembrane trafficking or the actin cytoskeleton, then examined pollen tube growth using fluorescent protein markers that label transport vesicles, endosomes, or the actin cytoskeleton. Both brefeldin A (BFA) and wortmannin disturbed the motility and structural integrity of ARA7- but not ARA6-labeled endosomes, suggesting heterogeneity of the endosomal populations. Disrupting endomembrane trafficking by BFA or wortmannin perturbed actin polymerization at the apical region but not in the longitudinal actin cables in the shank. The interference of BFA/wortmannin with actin polymerization was progressive rather than rapid, suggesting an indirect effect, possibly due to perturbed endomembrane trafficking of certain membrane-localized signaling proteins. Both the actin depolymerization drug latrunculin B and the actin stabilization drug jasplakinolide rapidly disrupted transport of secretory vesicles, but each drug caused distinct responses on different endosomal populations labeled by ARA6 or ARA7, indicating that a dynamic actin cytoskeleton was critical for some steps in endomembrane trafficking. Our results provide evidence of cross talk between endomembrane trafficking and the actin cytoskeleton in pollen tubes.

Pollen tubes of flowering plants are specialized cells that deliver immotile sperm to the proximity of female gametes for successful reproduction (Johnson and Preuss, 2002). The growth of pollen tubes is both polar and directional (Hepler et al., 2001); many cellular activities contribute to such growth, the most important being the dynamics of the actin cytoskeleton system, targeted exocytosis, and endocytosis (Hepler et al., 2001).

Pollen tubes contain longitudinal actin cables along the shank, which are important for providing structural support and acting as tracks for the movement of large organelles (Staiger et al., 1994). The apical area of pollen tubes instead contains dynamic filamentous actin (F-actin), as shown by fluorescently labeled actin-binding proteins (Kost et al., 1999; Fu et al., 2001; Chen et al., 2002; Wilsen et al., 2006). The dynamics of F-actin are critical for the polarized growth of pollen tubes. Genetically manipulating the activities of the small GTPases ROP (Kost et al., 1999; Fu et al., 2001; Cheung et al., 2008) and Rab (de Graaf et al., 2005), or of actin-binding proteins such as profilin and formin (Staiger et al., 1994; Chen et al., 2002; Cheung and Wu, 2004), disrupted F-actin dynamics and inhibited tube growth and caused apical bulges. Application of drugs such as latrunculin B (LatB) and jasplakinolide (Jas) showed similar effects (Gibbon et al., 1999; Vidali et al., 2001; Cardenas et al., 2005; Hörmanseder et al., 2005; Chen et al., 2007).

Targeted exocytosis delivers building materials for cell membranes and cell walls and therefore is critical for maintaining growth polarity and directionality of growing pollen tubes (Hepler et al., 2001). Because targeted exocytosis brings more membrane and wall materials than needed to the apex of a pollen tube, an active endocytic system exists to retrieve excess secreted materials. In addition to this nonselective bulk

¹ This work was supported by the U.S. Department of Agriculture-Agricultural Research Service Current Research Information System (grant no. 5335-21000-030-00D) and by the United States-Israel Binational Agricultural Research and Development Fund (grant no. IS4032-07). J.H. was partly supported by the West China Human Resource Development Program.

² These authors contributed equally to the article.

* Corresponding author; e-mail sheilamc@berkeley.edu.

The author responsible for distribution of materials integral to the findings presented in this article in accordance with the policy described in the Instructions for Authors (www.plantphysiol.org) is: Sheila McCormick (sheilamc@berkeley.edu).

[C] Some figures in this article are displayed in color online but in black and white in the print edition.

[W] The online version of this article contains Web-only data.

[OA] Open Access articles can be viewed online without a subscription.

www.plantphysiol.org/cgi/doi/10.1104/pp.109.142349

membrane retrieval, pollen tubes may have selective and regulated endocytic trafficking pathways. For example, experiments using charged gold particles indicated the existence of two distinct endocytic pathways in tobacco (*Nicotiana tabacum*) pollen tubes (Moscatelli et al., 2007), and other studies showed that pollen tubes are able to take in materials from the extracellular matrix (Lind et al., 1996; Goldraij et al., 2006). The axis of targeted exocytosis correlated with the direction of tube growth and it asymmetrically changed toward the new apex during tube reorientation (Camacho and Malho, 2003; de Graaf et al., 2005). Disruption of membrane trafficking altered growth trajectories (de Graaf et al., 2005). Both suggest that membrane trafficking is a critical part of polarity maintenance and reorientation.

As two important cellular processes in pollen tube growth, membrane trafficking and actin polymerization are conceivably dependent on each other. For example, several studies demonstrated that dynamic actin polymerization was essential for membrane trafficking (Hörmanseder et al., 2005; Wang et al., 2005; Chen et al., 2007; Lee et al., 2008), while others explored whether membrane trafficking affected actin polymerization (de Graaf et al., 2005; Hörmanseder et al., 2005). These studies, however, were mostly done with rapidly growing pollen tubes from tobacco or lily (*Lilium longiflorum*). For the model plant *Arabidopsis* (*Arabidopsis thaliana*), whose pollen tubes grow slower, little is known in this regard. Given a robust protocol for *Arabidopsis* pollen germination (Boavida and McCormick, 2007), it is now possible to investigate the interactions between these two cellular activities.

In this study, we analyzed the effects of drug treatments on *Arabidopsis* pollen tubes expressing fluorescent protein probes for transport vesicles, endosomes, or the actin cytoskeleton. We show that perturbing actin dynamics by LatB or Jas treatments disrupted the V-shaped distribution of transport vesicles, caused aggregation, and finally dissipation of a subpopulation of endosomes, indicating that actin dynamics are critical at some steps of endomembrane trafficking. On the other hand, disturbing endomembrane trafficking with brefeldin A (BFA) or wortmannin abolished the F-actin structure at the apical region without affecting the longitudinal actin cables at the shank. These results provide evidence that endomembrane trafficking and actin dynamics interact at certain steps during polarized growth of *Arabidopsis* pollen tubes.

RESULTS AND DISCUSSION

Optimization of Pharmacological Treatments on *Arabidopsis* Pollen Tube Growth

Inhibitors perturb cellular processes and thereby are useful for understanding their mechanisms. BFA is a fungal toxin that interferes with the activity of Arf guanine nucleotide exchange factors and thereby interferes with endomembrane trafficking (Nebenfuhr et al., 2002).

Wortmannin inhibits the activity of phosphatidylinositol 3-P kinase and therefore disturbs phosphatidylinositol 3-P production and possibly its distribution, which is critical for endomembrane trafficking (van Leeuwen et al., 2004). Wortmannin at high concentrations (above 30 μM) also inhibited phosphatidylinositol-4-phosphate (PI4P) and phosphatidylinositol-4,5-bisphosphate [PI(4,5)P₂] production by inhibiting type III PI4 kinase (Krinke et al., 2007). Because PI4P and PI(4,5)P₂ regulate both vesicle trafficking and the actin cytoskeleton in animal cells (Balla and Balla, 2006), we were concerned that wortmannin treatment might not be specific. Therefore we used a concentration well below 30 μM , to minimize interference with the actin cytoskeleton or with PI4P and PI(4,5)P₂ production. Studies with tobacco BY2 cells as well as with *Arabidopsis* seedlings showed that wortmannin treatment below 30 μM did not obviously affect the PI4P level, as shown by a fluorescent-tagged PI4P probe, PH_{FAPP1} (Vermeer et al., 2009). LatB depolymerizes the actin cytoskeleton (Gibbon et al., 1999) while Jas stabilizes it (Cardenas et al., 2005). Except for wortmannin, these other inhibitors have been used in pollen tubes of various species such as pea (*Pisum sativum*), lily, and tobacco, where they resulted in growth arrest and tube bulges (Gibbon et al., 1999; Vidali et al., 2001; Cardenas et al., 2005; de Graaf et al., 2005; Wang et al., 2005; Wilsen et al., 2006; Chen et al., 2007; Lovy-Wheeler et al., 2007). Because pollen tubes from different plant species may have distinct sensitivities toward pharmacological drugs, optimized concentrations for *Arabidopsis* had to be determined. To examine the dynamic changes of endomembrane trafficking as well as actin polymerization, we used inhibitor concentrations that disturb these cellular activities without causing cell death. At such concentrations, the effects of inhibitor treatment, as assessed by reductions in growth rate and increases in tube width, could be visualized over time.

We applied serial dilutions of different inhibitors based on concentrations in previous reports (Gibbon et al., 1999; Vidali et al., 2001; Cardenas et al., 2005; de Graaf et al., 2005; Wang et al., 2005; Wilsen et al., 2006; Chen et al., 2007; Lovy-Wheeler et al., 2007). Because inhibitors were dissolved in dimethyl sulfoxide (DMSO), we also confirmed that adding equivalent volumes of DMSO to control tubes had no phenotypic consequences over the time course of the experiments. Inhibitors were added 4 h after pollen germination in liquid germination medium (pollen germination medium [PGM]). Several concentrations of BFA were used: There was hardly any effect on tube growth rate or width at 0.7 μM or 1 μM (Fig. 1C), however, at 1.4 μM inhibitory effects, i.e. reduced growth rate and increased tube width, became obvious (Fig. 1C). Tube width and growth rate were not more affected at higher concentrations (i.e. 3 μM), suggesting that there is a threshold for inhibitory effects of BFA. Threshold concentrations were also identified for LatB and Jas. Treatment with LatB and Jas both resulted in tube

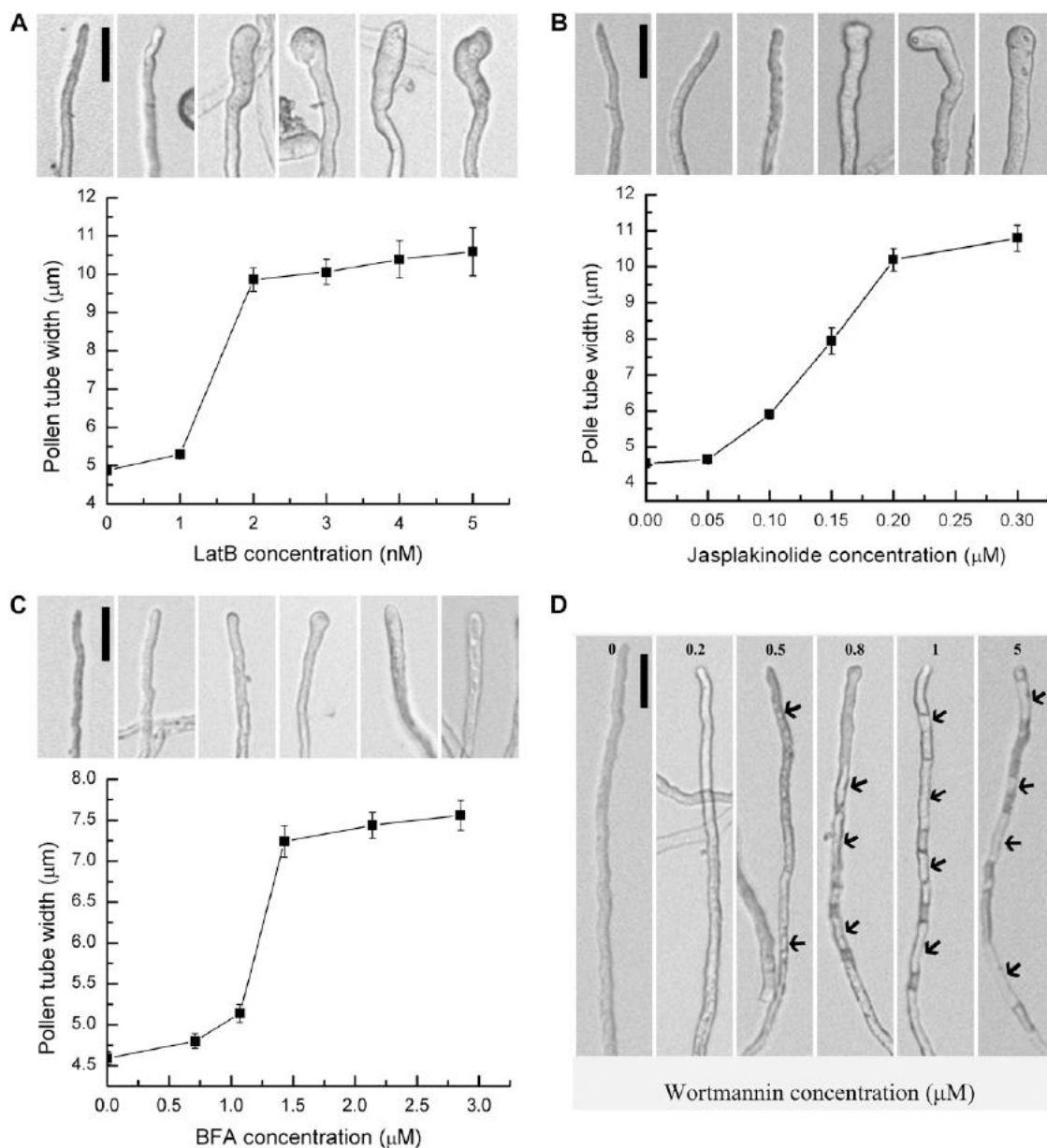


Figure 1. Optimization of pharmacological treatments for Arabidopsis pollen tubes. Pollen tube width was measured, or vacuoles were noted. A representative image for each concentration is shown above the graph. A, LatB treatment. B, Jas treatment. C, BFA treatment. D, Wortmannin treatment. Arrows indicate vacuoles. Scale bars = 50 μm .

bulging and growth arrest at high concentrations (Fig. 1, A and B). LatB at 1 to 2 nM and Jas at 0.1 to 0.2 μM showed a steeply increasing effect on pollen tube width (Fig. 1, A and B). The increased tube width upon application of BFA, LatB, and Jas suggested that these drugs compromised tube polarity. In contrast, the most prominent phenotypic effect upon wortmannin treatment was increased vacuolation. After treatment with 0.5 μM wortmannin, vacuoles were observed 50 μm from the apex (Fig. 1D). Concentrations of 0.5 μM , 0.8 μM , and 1 μM caused increased vacuolation and the vacuoles were closer to the apex (Fig. 1D). Concentrations higher than 1 μM (5 μM and

10 μM were tested) did not show obvious differences from 1 μM .

Based on these results, we chose 1.4 μM BFA, 2 nM LatB, 0.15 μM Jas, and 0.8 μM wortmannin for subsequent experiments.

Generation of Stable Transgenic Arabidopsis Expressing Pollen-Specific Fluorescent Protein Markers

To study the dynamics of endomembrane trafficking and actin polymerization in Arabidopsis pollen tubes, we generated constructs expressing yellow fluorescent

protein (YFP)-fused markers. Arabidopsis RabA4b was used as the marker for transport vesicles. RabA4b is a Rab GTPase specifically localized at an inverted cone-shaped area in the apical region of both tobacco pollen tubes (Lee et al., 2008) and Arabidopsis root hairs (Preuss et al., 2004). Two other Rab GTPases, ARA6 and ARA7, were used as markers for endosomes, although neither has been used before in pollen tubes. Although it is unequivocal that both ARA6 and ARA7 label endosomes, different groups differed as to the type of endosomes they label, either early endosomes, later endosomes, or prevacuolar compartments (Ueda et al., 2001, 2004; Tse et al., 2004).

We used YFP-fused mouse talin (YFP-mTalin) as the marker for the actin cytoskeleton. Although studies have shown that mTalin bundles actin and therefore affects organization of the actin cytoskeleton (Ketelaar et al., 2004; Wilsen et al., 2006), it has been used in pollen tubes to demonstrate the dynamics of F-actin at the apical clear zone (Kost et al., 1999; Fu et al., 2001). We found that strong expression of mTalin indeed bundled actin microfilaments and caused tubes to bulge (data not shown). However, moderate expression of YFP-mTalin did not cause growth inhibition or changes of tube morphology (Fig. 2).

We first tested these fluorescent markers in tobacco pollen using particle bombardment. As expected, YFP-RabA4b formed an inverted cone shape in the apical cytoplasm and a longitudinal tail in the center of pollen tubes (Supplemental Fig. S1A). This localization resembled that of tobacco Rab11 (de Graaf et al., 2005) and thus indicates where transport vesicles are. ARA6 and ARA7 both labeled punctate, highly motile vesicular structures (Supplemental Fig. S1, B and C) characteristic of endosomes (Cheung and Wu, 2007). However, ARA7-labeled endosomes were present not only in the tube shank but also in the apical clear zone (Supplemental Fig. S1C), whereas ARA6-labeled endosomes were excluded from the apical clear zone (Supplemental Fig. S1B). Such distinct localizations suggested that ARA6 and ARA7 label different populations of endosomes in pollen tubes. Recently two distinct endocytic pathways were proposed to occur in pollen tubes, one at the very apex and the other at the subapical region (Zonia and Munnik, 2009). The distinct distribution of ARA6- and ARA7-labeled endosomes may reflect such a spatial separation of endocytic pathways. YFP-mTalin (Supplemental Fig. S1D) labeled longitudinal or slightly helical cables along the tube shank as well as an F-actin collar/ring at the junction between the apical and subapical region, as previously described (Kost et al., 1999; Fu et al., 2001).

Having established the validity of these fluorescent markers, we then generated stable transgenic Arabidopsis plants in the *quartet1* background. For each construct we obtained more than 50 individual T1 lines and selected 10 lines having single T-DNA insertions, based on the criterion that two of the four grains in a given quartet showed fluorescence. Homozygous T3 plants were used for subsequent analyses.

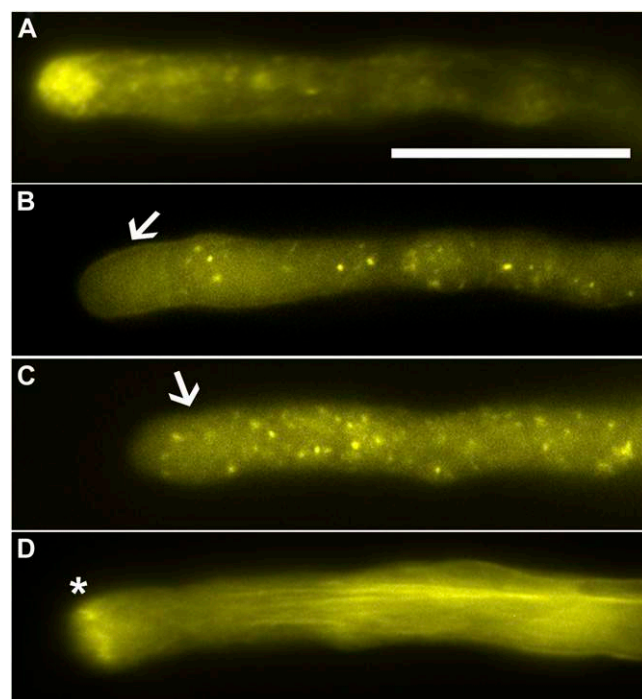


Figure 2. Fluorescent probes for transport vesicles, endosomes, and the actin cytoskeleton expressed in transgenic Arabidopsis pollen tubes. A, A pollen tube expressing YFP-RabA4b. B, A pollen tube expressing ARA6-YFP. C, A pollen tube expressing YFP-ARA7. D, A pollen tube expressing YFP-mTalin. Arrows in B and C indicate the apical clear zone, in which ARA6-labeled endosomes are excluded while ARA7-labeled endosomes are present. Asterisk in D marks the apical F-actin ring. Scale bar = 20 μm . [See online article for color version of this figure.]

The subcellular localization of RabA4b (Fig. 2A) and mTalin (Fig. 2D) in Arabidopsis pollen tubes was the same as in tobacco pollen tubes. The distinction between ARA6- and ARA7-labeled endosomes regarding whether they were present in the clear zone was less obvious but still distinguishable (Fig. 2, B and C). In addition to endosome localization, ARA6 was detected at the plasma membrane of pollen tubes and on the invaginated vegetative cell plasma membrane surrounding the sperm cells in transgenic lines that had high expression levels (data not shown). This plasma membrane localization of ARA6 may result from its reported *N*-myristoylation and palmitoylation (Ueda et al., 2001).

To verify that the expression of these fusion proteins did not perturb tube growth and morphology, we measured pollen tube width and growth rates during *in vitro* pollen germination assays. There was no significant difference between pollen tubes expressing these fusion proteins and wild-type pollen tubes, either in tube width or in growth rate (Supplemental Fig. S2), indicating that the expression of these fusion proteins did not disturb normal cellular activities in pollen tubes.

Disturbance of Transport Vesicles and Endosomes by BFA and Wortmannin Treatment

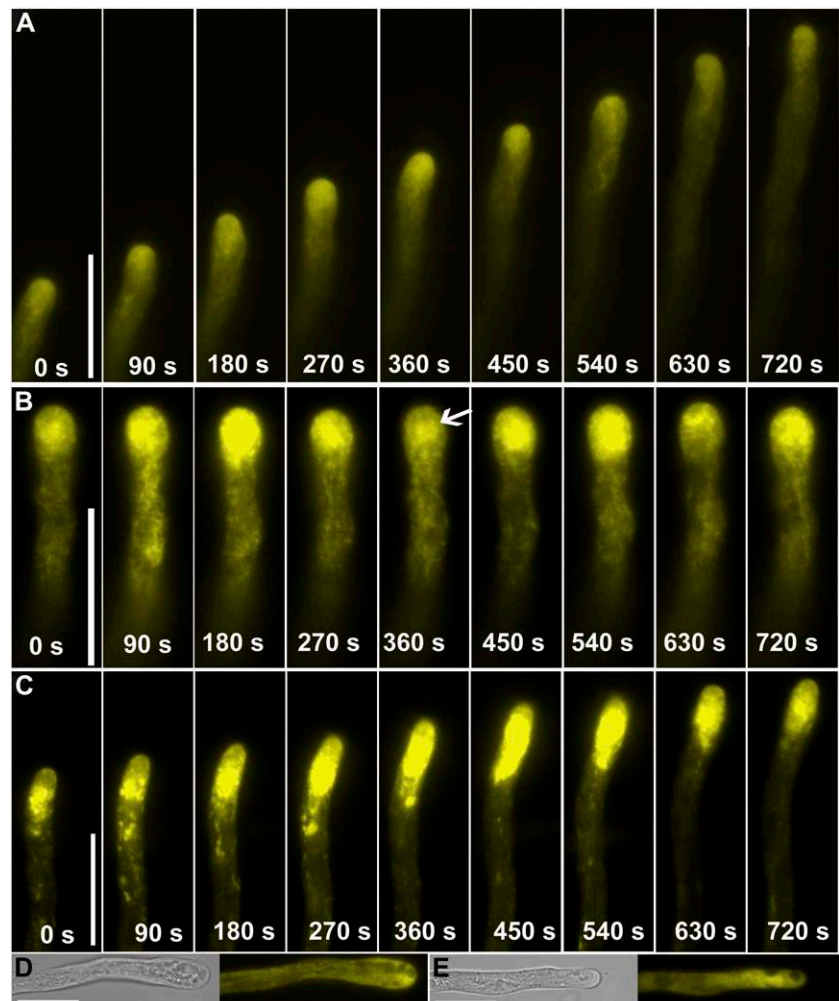
In control pollen tubes, transport vesicles labeled by RabA4b accumulated in an inverted cone-shaped region in the apical cytoplasm (Fig. 2A). The axis of such inverted cones changed to a new growth direction during tube reorientation (Fig. 3A; Supplemental Movie S1), as did that of NtRab11 (de Graaf et al., 2005), suggesting that the directional movement of transport vesicles is part of the reorientation process during tube growth. Often, longitudinal RabA4b labeling could be seen in the center of pollen tubes (Fig. 3A), which may indicate the path of cytoplasmic streaming.

After 5 min incubation with BFA, pollen tubes continued growth and RabA4b localization resembled the pattern in control tubes (data not shown). At around 20 min, tube growth slowed down, and this was accompanied by increased fluorescence intensity in the apical cytoplasm (Fig. 3B). BFA inhibits exocytosis but may increase endocytosis (Wang et al., 2005), which explains the increased signal intensity after a short incubation with BFA. The fluorescence intensity increase appeared to oscillate, although pollen tubes

had almost stopped growth (Fig. 3B; Supplemental Movie S2). The YFP accumulation zone was shifted from the very apical region to the subapical area (Fig. 3B) and the YFP label formed aggregates resembling the so-called BFA-induced aggregates (BIA) that were previously described in tobacco pollen tubes (Parton et al., 2001, 2003). Prolonged BFA treatment (60–90 min) caused apical bulges and growth arrest, with vacuoles invading the apical region and an absence of the typical V-shaped RabA4b labeling (Fig. 3D). The fluorescence was evenly distributed in the cytoplasm (Fig. 3D), indicating that directional vesicle transport had stopped.

Wortmannin did not affect the V-shaped localization of RabA4b within the first 45 min of treatment (data not shown), but after 60 min the RabA4b labeling shifted backwards to the junction between the apical and subapical region (Fig. 3C), and this was correlated with slowed growth. RabA4b labeling was in distinct motile patches in the apical and subapical area (Fig. 3C; Supplemental Movie S3). Unlike treatment with BFA, wortmannin-treated tubes did not show an oscillating fluorescence pattern (Fig. 3C). Further incu-

Figure 3. Time-lapse images of transgenic pollen tubes expressing YFP-RabA4b. A, Control. B, A pollen tube treated with BFA. Arrow indicates the RabA4b labeling below apex after BFA treatment, which resembles so-called BIA. Serial images were taken starting after 20 min incubation with BFA. Therefore time point 0 s is after 20 min treatment with BFA. C, A pollen tube treated with wortmannin. Serial images were taken starting after 60 min incubation with wortmannin. Therefore time point 0 s is after 60 min treatment with wortmannin. D, A representative pollen tube treated with BFA for 60 min. E, A representative pollen tube treated with wortmannin for 90 min. For D and E, left section, transmitted light; right section, YFP channel. Scale bars = 20 μ m. [See online article for color version of this figure.]



bation resulted in vacuolation at the apical region and caused redistribution of the RabA4b signal to the cytoplasm (Fig. 3E).

To confirm these results, we also applied FM4-64, a lipophilic dye that labels vesicles via endocytosis, to RabA4b-labeled tubes treated with either BFA (Supplemental Fig. S3) or wortmannin (Supplemental Fig. S4). BFA treatment increased FM4-64 uptake into pollen tubes. Treatment with BFA disrupted the distribution pattern of both RabA4b-labeled and FM4-64-labeled transport vesicles and formed BIAs (Supplemental Fig. S3). In contrast, although wortmannin also disrupted the distribution pattern of transport vesicles labeled by both RabA4b and FM4-64, pretreatment with wortmannin inhibited FM4-64 uptake (Supplemental Fig. S4). The RabA4b signal overlapped with the FM4-64 signal at the apical region but not at the pollen tube shank (Supplemental Fig. S4).

ARA7-labeled endosomes were fast-moving punctuate vesicles detected throughout pollen tubes and including the apical clear zone (Fig. 2C). A 30 min incubation with BFA caused aggregation of ARA7-labeled endosomes (Fig. 4A), which were distinct from the ring-shaped compartments that ARA7-labeled endosomes formed upon BFA treatment or in protoplasts prepared from the Arabidopsis *gnom* mutant (Geldner et al., 2003). This may indicate a cell-specific endosomal response to BFA. ARA7 labeling dissipated into the cytoplasm after prolonged (60–90 min) BFA incubation (Fig. 4A), when growth was arrested.

Incubation with wortmannin did not affect the localization pattern and motility of ARA7-labeled endosomes within the first 30 min (data not shown), consistent with the normal tube morphology and

growth rate. However, ARA7-labeled endosomes started to form large aggregates after 45 min incubation with wortmannin (Supplemental Movie S4); 90 min incubation resulted in vacuolation at the apex and growth arrest, when a few large aggregates were labeled by ARA7 (Fig. 4B).

Surprisingly, ARA6-labeled endosomes showed responses distinct from those of ARA7-labeled endosomes, with both BFA and wortmannin treatments. The ARA6 signal was seen at punctate motile vesicles in the cytoplasm (Fig. 2B; Supplemental Movie S5). BFA treatment depleted ARA6 from the apical plasma membrane (Fig. 4C), likely a result of inhibited exocytosis, which is a well-documented effect of BFA treatment (Nebenfuhr et al., 2002; Geldner, 2004). However, ARA6-labeled endosomes did not aggregate, even after prolonged BFA treatment (Fig. 4C). ARA6-labeled endosomes penetrated the apical clear zone upon BFA treatment (Fig. 4C; Supplemental Movie S5) where they were usually excluded, indicating disrupted cellular structures due to BFA treatment. ARA6-labeled endosomes were less numerous after prolonged BFA treatment (Fig. 4C). Previous studies in Arabidopsis protoplasts were contradictory regarding the sensitivity of ARA6-labeled endosomes to BFA (Grebe et al., 2003; Ueda et al., 2004). That ARA6-labeled endosomes were BFA insensitive was previously indicated, in that they were not affected in the *gnom* mutant, in which a BFA-sensitive Arf guanine nucleotide exchange factors is defective (Geldner et al., 2003). Our data showed that in pollen tubes ARA6-labeled endosomes are BFA insensitive.

Wortmannin treatment also did not affect the morphology or motility of ARA6-labeled endosomes (Fig. 4D). Only when pollen tubes were incubated with wortmannin for more than 60 min did ARA6-labeled endosomes start to aggregate (Fig. 4D), although to a much lesser extent than for ARA7-labeled aggregates (Fig. 4B). In tubes treated with wortmannin for more than 80 min, when tubes were highly vacuolated, ARA6 occasionally accumulated at ring-shaped compartments (Fig. 4D). That ARA7- and ARA6-labeled endosomes showed different responses to BFA and wortmannin suggests that they are distinct subpopulations of endosomes.

Because both BFA and wortmannin treatments disrupted the FM4-64 distribution pattern, we labeled ARA7- or ARA6-expressing tubes with FM4-64 to verify the treatments with these two drugs. Indeed, disturbance of the FM4-64-labeling pattern upon BFA or wortmannin treatments correlated with the aggregation of ARA7-labeled endosomes but not of ARA6-labeled endosomes (Supplemental Figs. S5 and S6). Furthermore, we generated transgenic plants coexpressing ARA6-CFP and YFP-ARA7 and treated these transgenic pollen tubes with either BFA or wortmannin. As expected, ARA7- and ARA6-labeled endosomes showed different responses to BFA and wortmannin (Supplemental Fig. S7), strongly supporting the heterogeneity of endosomes in pollen tubes.

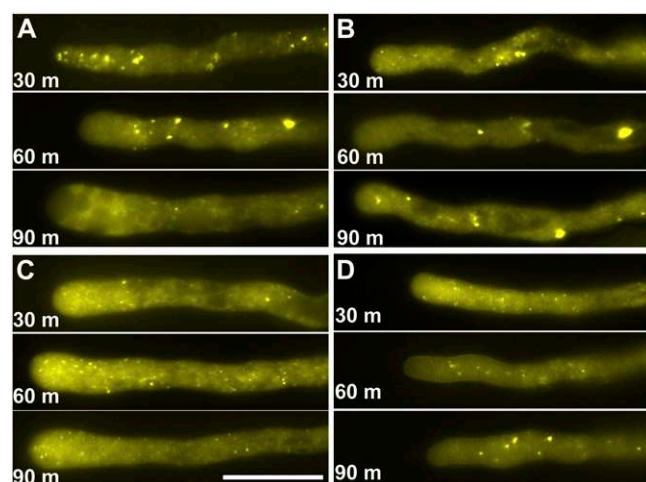


Figure 4. Endosomes respond differently to BFA and wortmannin. A, Pollen tubes expressing YFP-ARA7 treated with BFA. B, Pollen tubes expressing YFP-ARA7 treated with wortmannin. C, Pollen tubes expressing YFP-ARA6 treated with BFA. D, Pollen tubes expressing YFP-ARA6 treated with wortmannin. The images shown are representative, chosen from more than 30 pollen tubes at each time point (30, 60, and 90 min). Scale bars = 20 μ m. [See online article for color version of this figure.]

The Effects of LatB and Jas Treatments on Transport Vesicles and Endosomes in Arabidopsis Pollen Tubes

The effects of LatB treatment on the dynamics of the actin cytoskeleton have been extensively studied with pollen tubes of several plant species (Fu et al., 2001; Vidali et al., 2001; Chen et al., 2002, 2007). We obtained similar results with Arabidopsis pollen tubes. A 30 min incubation with LatB disrupted the apical F-actin ring structure (Supplemental Fig. S8A), and after 60 min ectopic actin cables penetrated the apical region (Supplemental Fig. S8B). Application of Jas disrupted actin cables along the tube shank (Supplemental Fig. S8C) within 10 min, and resulted in enrichment of short, thick actin patches beneath the plasma membrane (Supplemental Fig. S8D), as reported for lily pollen tubes (Cardenas et al., 2005).

To find out how the dynamics of the actin cytoskeleton affected the dynamics of transport vesicles in Arabidopsis pollen tubes, we applied LatB or Jas to tubes expressing RabA4b-YFP. LatB treatment caused rapid relocation of the inverted cone labeled by RabA4b backward from the very apex, forming a patch at the subapical region (Fig. 5A). Further incubation with LatB caused dissipation of the RabA4b signal, resulting in an even cytoplasmic distribution and growth arrest (Supplemental Movie S6). These results are consistent with the dissipation of the RabA4b signal to the cytoplasm and with the cessation of root hair growth seen upon treatment with 200 nM LatB (Preuss et al., 2004). The RabA4b signal was fragmented upon treatment with Jas (Fig. 5B). Because Jas treatment caused fragmentation of actin cables at the shank and aggregation of actin microfilaments at

the apical region (Supplemental Fig. S8, C and D), the fragmented RabA4b signal upon Jas treatment indicates that transport vesicles in pollen tubes require an intact actin cytoskeleton for directional movement. Further incubation with Jas redistributed the RabA4b signal evenly in the cytoplasm (data not shown). These results support the idea that a dynamic actin cytoskeleton is critical for the trafficking of transport vesicles.

Endosomes labeled by ARA6 or ARA7 showed distinct responses to LatB and Jas. ARA7-labeled endosomes started to form large aggregates after 10 min incubation with LatB (data not shown), which were more obvious after 30 min incubation (Fig. 6A). However, such aggregates were few, reduced in motility, and persisted in tubes that had been treated with LatB for 60 min, when growth was already arrested (Fig. 6A). Jas treatment had similar aggregation effects on ARA7-labeled endosomes (Fig. 6B). However, prolonged (60 min) Jas treatment caused dissipation of the ARA7 signal from these aggregates to an even cytoplasmic distribution (Fig. 6B). In contrast, ARA6-labeled endosomes were insensitive to both Jas and LatB treatments and no obvious aggregation was seen (Fig. 6, C and D), although they penetrated to the apical region (Fig. 6, C and D) where they were excluded in control tubes (Fig. 2B). These results indicated that a dynamic actin cytoskeleton is critical for certain steps during endocytic routes that affect a subpopulation of endosomes.

The Effects of BFA and Wortmannin Treatments on the Dynamics of Actin Cytoskeleton

In contrast to the regulation of endomembrane trafficking by the actin cytoskeleton, few studies have been done to explore whether and how endomembrane trafficking affects actin dynamics during tube growth (de Graaf et al., 2005; Hörmanseder et al., 2005). Expression of either a dominant negative or constitutively active version of NtRab11b abolished the apical actin ring structure without disrupting actin cables in the shank (de Graaf et al., 2005), suggesting that transport vesicles influence actin dynamics. In addition, BFA treatment of lily pollen tubes caused association of a so-called actin basket with BIA, on which organelles move between the plasma membrane and BIA (Hörmanseder et al., 2005).

To find out how perturbing endomembrane trafficking affected the actin cytoskeleton, we applied either BFA or wortmannin to tubes expressing mTalin. Because we established the effects of BFA or wortmannin on endomembrane trafficking, the dynamics of the actin cytoskeleton after these drug treatments should reflect its response to perturbed endomembrane trafficking. Incubation with BFA for 5 min did not change the actin cables in the shank or the F-actin ring at the apex (data not shown). After 20 min, when BFA treatment affected tube growth as expected (i.e. an increased apical dome and a disrupted clear zone was seen), the apical F-actin ring disappeared while actin

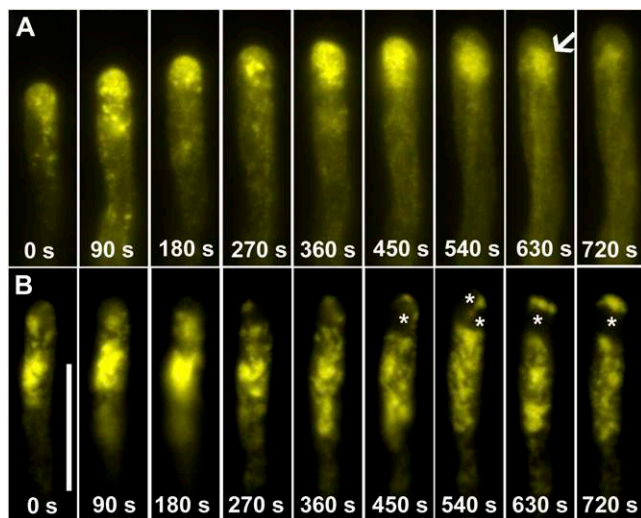


Figure 5. Time-lapse images of transgenic pollen tubes expressing YFP-RabA4b. A, A pollen tube treated with LatB for 15 min. Arrow indicates RabA4b labeling below apex, which resembles the so-called BIA. B, A pollen tube treated with Jas for 15 min. Asterisks indicate vacuoles. Scale bar = 20 μ m. Serial images were taken starting after 15 min incubation with LatB (A) or Jas (B). Therefore time point 0 s is after 15 min treatment with the drugs. [See online article for color version of this figure.]

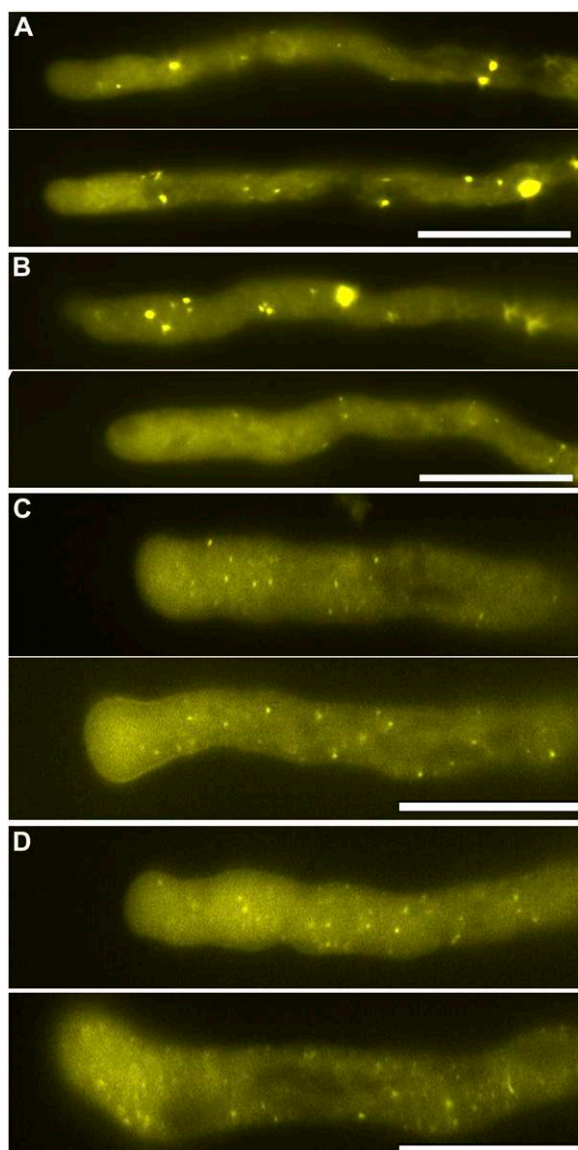


Figure 6. Dynamic actin polymerization regulates ARA7- but not ARA6-labeled endosomes. A and B, Pollen tubes expressing YFP-ARA7. C and D, Pollen tubes expressing YFP-ARA6. A and C, LatB treatment for 30 min (top section) or 60 min (bottom section). B and D, Jas treatment for 30 min (top section) and 60 min (bottom section). The images shown are representative, chosen from more than 30 pollen tubes at each time point (30 and 60 min). Scale bar = 20 μ m. [See online article for color version of this figure.]

cables at the tube shank were still intact (Fig. 7A). Tangled actin cables penetrated to the apical region and surrounded small vacuoles in the apex (Fig. 7A). However, these actin cable structures disappeared after prolonged (60 min) incubation with BFA, when a large vacuole occupied the apex and growth was arrested (Fig. 7A).

The effect of wortmannin on the actin cytoskeleton was slower, in that 45 min incubation did not change either the F-actin ring at the apex or the actin cables in

the shank (Fig. 7B). After 60 min, however, the actin ring disappeared (Fig. 7B). Instead, a strong fluorescent labeling of tangled actin cable structures was detected below the apex (Fig. 7B), similar to the previously reported BIA-associated actin structures (Hörmanseder et al., 2005). Prolonged (90 min) treatment with wortmannin caused tube vacuolation at the apex and the actin cables penetrated the apex, surrounded the vacuole, and were also tangled beneath the apical plasma membrane (Fig. 7B). Both drugs caused disappearance of the F-actin ring at the apex, suggesting that this F-actin ring is sensitive to perturbations of endomembrane trafficking.

Interdependency of Actin Dynamics and Endomembrane Trafficking in Pollen Tubes

A dynamic actin cytoskeleton and regulated endomembrane trafficking are two critical cellular activities leading to polarized growth of pollen tubes (Hepler et al., 2001). We show here using pharmacological

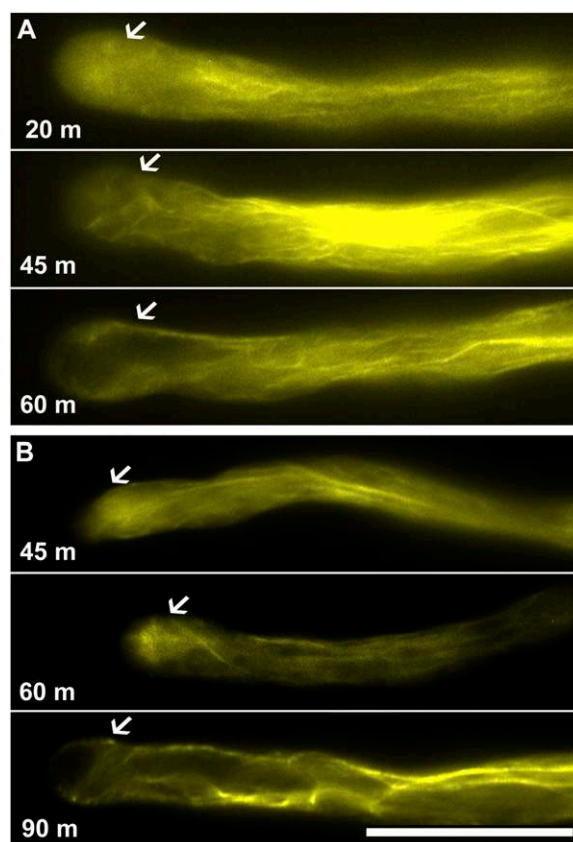


Figure 7. Apical F-actin, but not actin cables in the shank, is sensitive to disturbances of endomembrane trafficking. A, BFA treatment. B, Wortmannin treatment. The images shown are representative, chosen from more than 30 pollen tubes at each time point (for BFA: 20, 45, and 60 min; for wortmannin: 45, 60, and 90 min). Arrows indicate where the F-actin ring would be in control tubes. Scale bar = 20 μ m. [See online article for color version of this figure.]

drugs that these two cellular activities are interdependent in *Arabidopsis* pollen tubes.

A dynamic actin cytoskeleton at the apex, as reflected by the presence of the F-actin ring, was critical for the directional movement of transport vesicles to the tip, based on the effects of LatB and Jas on spatiotemporal RabA4b distribution (Fig. 5). A dynamic actin cytoskeleton is essential for endomembrane trafficking involving ARA7-labeled endosomes but not ARA6-labeled endosomes, in that ARA7- but not ARA6-labeled endosomes quickly became immotile and aggregated in the presence of LatB or Jas (Fig. 6). ARA7 most likely labels an early endosome population (Ueda et al., 2004) and/or vesicles immediately exiting the trans-Golgi network, which were also considered early endosomes (Samaj et al., 2006). Indeed, it was reported that early endosomes, but not late endosomes or prevacuolar compartments, are sensitive to BFA (Tse et al., 2004; Ueda et al., 2004). Our results showing that ARA6-labeled endosomes are insensitive to BFA and wortmannin suggested that ARA6 localized at late endosomes or prevacuolar compartments in pollen tubes (Fig. 4; Supplemental Figs. S5 and S6). That ARA6-labeled endosomes were excluded from the apical clear zone (Fig. 2; Supplemental Fig. S1), where ARA7-labeled endosomes were present, further suggests that ARA7-labeled endosomes are early endosomes, where membrane protein recycling and sorting occur. We used double-labeling experiments to indicate the heterogeneity of the endosome populations labeled by ARA6 or ARA7 (Supplemental Fig. S7). Because fluorescence microscopy has limited resolution, ultrastructural studies should be used to confirm these findings.

On the other hand, disturbing endomembrane trafficking by BFA or wortmannin disrupted the apical F-actin ring at the apex without affecting actin cables in the shank. Such an effect was delayed and progressive and therefore might have resulted from an altered membrane presence of signaling proteins. Plausible candidates for such signaling proteins are ROP GTPases. ROP GTPases regulate dynamic actin polymerization in pollen tubes (Fu et al., 2001), and both in pollen tubes and in sporophytic cells they also regulate membrane trafficking through actin dynamics and/or their effectors (Lavy et al., 2007; Lee et al., 2008). ROP-GTP is spatiotemporally restricted to the apical plasma membrane (Wu et al., 2001) by the coordinated function of a receptor kinase (PRK2a) and a ROP guanine nucleotide exchange factor (Zhang and McCormick, 2007), suggesting that ROP-mediated signaling is a convergence point for actin dynamics and endomembrane trafficking in pollen tubes.

MATERIALS AND METHODS

Generation of Stable Transgenic Protein Fusion Marker Lines

The expression construct for mTalin (Zhang et al., 2009) was described previously. RabA4b, ARA6, and ARA7 were PCR amplified from inflorescence

cDNA and ligated into a pENTRY/D-TOPO vector to generate entry vectors using the following primer pairs: for RabA4b (At4g39990), 5' CACCATG-GCCGGAGGAGGC3' and 5TCAAGAAGAAGTACAACAAGTGTCTG3'; for ARA6 (At3g54840), 5' CACCATGGGATGTGCTTCTTCTTCCA3' and 5'TGACGAAGGAGCAGGACGAGGT3'; for ARA7 (At4g19640), 5' CACCA-TGGCTGCAGCTGGAAACAAGA3' and 5'CTAAGCACAACAAGATGAG-CTCACTGC3'. The entry vectors for RabA4b, ARA6, and ARA7 were generated by TOPO ligation (Invitrogen) and verified by sequencing. The YFP and CFP fusion expression constructs were generated by LR reactions with previously described pollen-specific Gateway (Invitrogen) destination vectors (Zhang and McCormick, 2007). The *Arabidopsis thaliana* *quartet1-2* (*qrt1*) mutant in the Columbia-0 ecotype was used as wild type for stable transformation by the floral-dipping method (Clough and Bent, 1998). Transgenic plants were selected on Murashige and Skoog medium supplemented with 30 $\mu\text{g}/\text{mL}$ Basta, then transferred to soil in a 4:1:1 mix of Fafard 4P:perlite:vermiculite under an 18-h light/6-h dark cycle at 21°C.

Transient Expression in Tobacco Pollen Tubes by Particle Bombardment

Transient expression assays in tobacco (*Nicotiana tabacum*) pollen were as described (Zhang and McCormick, 2007). Images were captured from 4 to 8 h after germination.

Arabidopsis in Vitro Pollen Germination

Arabidopsis in vitro pollen germination was conducted at 22.5°C, as described (Boavida and McCormick, 2007). Briefly, liquid PGM (0.01% boric acid, 5 mM CaCl₂, 5 mM KCl, 1 mM MgSO₄) was always prepared fresh from 100× stock solutions using autoclaved MilliQ water (Millipore). Suc was added to a final concentration of 10% and the pH was adjusted to 7.8 using NaOH. For each liquid germination assay, 60 freshly opened flowers were placed in liquid PGM and agitated briefly on a vortex mixer. After removing flower parts with a forceps, the suspension was centrifuged at 2,000 rpm for 1 min to pellet pollen. Pollen grains were resuspended in 300 μL liquid PGM and transferred, using a cut-off pipette tip, to small (12 × 45 mm) glass vials for germination. Pollen tube width was measured at the widest region in the apical or subapical region, using the measuring function of Axiovision software. From 80 to 100 pollen tubes were measured to determine the average tube width and a *t* test was performed to determine if the difference was significant ($P < 0.05$, *t* test). The growth rate of pollen tubes was calculated from an average of the distance that 20 tubes grew in 15 min.

Pharmacological Treatments

Stock solutions of inhibitors (Calbiochem) were prepared in DMSO at the following concentrations: 357 μM BFA, 330 μM wortmannin, 5 mM LatB, and 1 mM Jas. Dilutions in DMSO were prepared and added in liquid PGM. DMSO was added to controls. For optimization of pharmacological treatments, pollen was germinated in liquid PGM for 4 h before adding inhibitors. Aliquots (50 μL) of germination medium with pollen were then distributed in individual wells of a 96-well micropipette plate. Inhibitors were added to individual wells, gently mixed, and then incubation was continued. To determine the effects of inhibitor treatments on the actin cytoskeleton and endomembrane trafficking, transgenic pollen expressing fluorescent protein markers was used. Inhibitors were added at a final concentration of 1.4 μM for BFA, 0.8 μM for wortmannin, 2 nM for LatB, or 0.15 μM for Jas. All experiments were repeated at least three times. A final concentration of 0.025 g/mL glutaraldehyde (Sigma) was added after 2 h incubation to fix the cells, before measuring pollen tube widths. FM4-64 (final concentration of 4 mM) was added to PGM 5 min before imaging. Images and movies shown are representative of approximately 30 pollen tubes observed for each experiment at different time points after drug treatment.

Microscopy

An inverted AxioPhot microscope (Zeiss) with either bright-field or epifluorescence optics was used. Images were captured using a Spot digital camera (Diagnostic Instruments), exported using AxioVision (Zeiss), and processed using Adobe Photoshop 7.0 (Adobe). All movies were generated using the 6D acquisition option, with 30 images taken at 30 s intervals.

Sequence data from this article can be found in the GenBank/EMBL data libraries under accession numbers AB007766 for ARA6, AB038491 for ARA7, and AY088624 for RabA4b.

Supplemental Data

The following materials are available in the online version of this article.

Supplemental Figure S1. Fluorescent protein probes expressed in tobacco pollen.

Supplemental Figure S2. Pollen tube morphology and growth rate in pollen-expressing fluorescent probes.

Supplemental Figure S3. Effect of BFA on transport vesicles labeled by YFP-RabA4b and FM4-64.

Supplemental Figure S4. Effect of wortmannin on transport vesicles labeled by YFP-RabA4b and FM4-64.

Supplemental Figure S5. Effect of BFA on pollen tubes expressing ARA6-YFP or YFP-ARA7 and labeled with FM4-64.

Supplemental Figure S6. Effect of wortmannin on pollen tubes expressing ARA6-YFP or YFP-ARA7 and labeled with FM4-64.

Supplemental Figure S7. Effects of BFA and wortmannin on pollen tubes coexpressing ARA6-CFP and YFP-ARA7.

Supplemental Figure S8. Effects of actin-disrupting drugs on YFP-mTalin labeling pattern.

Supplemental Movie S1. Transport vesicles labeled by YFP-RabA4b.

Supplemental Movie S2. Transport vesicles labeled by YFP-RabA4b in a BFA-treated pollen tube.

Supplemental Movie S3. Transport vesicles labeled by YFP-RabA4b in a wortmannin-treated pollen tube.

Supplemental Movie S4. ARA7-positive endosomes after wortmannin treatment.

Supplemental Movie S5. ARA6-positive endosomes after BFA treatment.

Supplemental Movie S6. Transport vesicles labeled by YFP-RabA4b in a LatB-treated pollen tube.

ACKNOWLEDGMENTS

We thank Leonor Boavida for helpful discussions, and Weihua Tang and Leonor Boavida for comments on the manuscript. We are grateful to University of California at Berkeley undergraduates Sarah Liu, James Pao, and Carolyn Jin for excellent technical assistance. We thank Shaul Yalovsky for a YFP-mTalin construct.

Received June 4, 2009; accepted February 19, 2010; published February 24, 2010.

LITERATURE CITED

- Balla A, Balla T** (2006) Phosphatidylinositol 4-kinases: old enzymes with emerging functions. *Trends Cell Biol* **16**: 351–361
- Boavida LC, McCormick S** (2007) Temperature as a determinant factor for increased and reproducible *in vitro* pollen germination in *Arabidopsis thaliana*. *Plant J* **52**: 570–582
- Camacho L, Malho R** (2003) Endo/exocytosis in the pollen tube apex is differentially regulated by Ca²⁺ and GTPases. *J Exp Bot* **54**: 83–92
- Cardenas L, Lovy-Wheeler A, Wilsen KL, Hepler PK** (2005) Actin polymerization promotes the reversal of streaming in the apex of pollen tubes. *Cell Motil Cytoskeleton* **61**: 112–127
- Chen CY, Wong EI, Vidali L, Estavillo A, Hepler PK, Wu HM, Cheung AY** (2002) The regulation of actin organization by actin-depolymerizing factor in elongating pollen tubes. *Plant Cell* **14**: 2175–2190
- Chen T, Teng N, Wu X, Wang Y, Tang W, Samaj J, Baluska F, Lin J** (2007)

- Disruption of actin filaments by Latrunculin B affects cell wall construction in *Picea meyeri* pollen tube by disturbing vesicle trafficking. *Plant Cell Physiol* **48**: 19–30
- Cheung AY, Duan QH, Costa SS, de Graaf BH, Di Stilio VS, Feijo J, Wu HM** (2008) The dynamic pollen tube cytoskeleton: live cell studies using actin-binding and microtubule-binding reporter proteins. *Mol Plant* **1**: 686–702
- Cheung AY, Wu HM** (2004) Overexpression of an *Arabidopsis* formin stimulates supernumerary actin cable formation from pollen tube cell membrane. *Plant Cell* **16**: 257–269
- Cheung AY, Wu HM** (2007) Structural and functional compartmentalization in pollen tubes. *J Exp Bot* **58**: 75–82
- Clough SJ, Bent AF** (1998) Floral dip: a simplified method for *Agrobacterium*-mediated transformation of *Arabidopsis thaliana*. *Plant J* **16**: 735–743
- de Graaf BH, Cheung AY, Andreyeva T, Levasseur K, Kieliszewski M, Wu HM** (2005) Rab11 GTPase-regulated membrane trafficking is crucial for tip-focused pollen tube growth in tobacco. *Plant Cell* **17**: 2564–2579
- Fu Y, Wu G, Yang Z** (2001) Rop GTPase-dependent dynamics of tip-localized F-actin controls tip growth in pollen tubes. *J Cell Biol* **152**: 1019–1032
- Geldner N** (2004) The plant endosomal system—its structure and role in signal transduction and plant development. *Planta* **219**: 547–560
- Geldner N, Anders N, Wolters H, Keicher J, Kronberger W, Muller P, Delbarre A, Ueda T, Nakano A, Jurgens G** (2003) The *Arabidopsis* GNOM ARF-GEF mediates endosomal recycling, auxin transport, and auxin-dependent plant growth. *Cell* **112**: 219–230
- Gibbon BC, Kovar DR, Staiger CJ** (1999) Latrunculin B has different effects on pollen germination and tube growth. *Plant Cell* **11**: 2349–2364
- Goldraij A, Kondo K, Lee CB, Hancock CN, Sivaguru M, Vazquez-Santana S, Kim S, Phillips TE, Cruz-Garcia F, McClure B** (2006) Compartmentalization of S-RNase and HT-B degradation in self-incompatible *Nicotiana*. *Nature* **439**: 805–810
- Grebe M, Xu J, Mobius W, Ueda T, Nakano A, Geuze HJ, Rook MB, Scheres B** (2003) *Arabidopsis* sterol endocytosis involves actin-mediated trafficking via ARA6-positive early endosomes. *Curr Biol* **13**: 1378–1387
- Hepler PK, Vidali L, Cheung AY** (2001) Polarized cell growth in higher plants. *Annu Rev Cell Dev Biol* **17**: 159–187
- Hörmanseder K, Obermeyer G, Foissner I** (2005) Disturbance of endomembrane trafficking by brefeldin A and calyculin A reorganizes the actin cytoskeleton of *Lilium longiflorum* pollen tubes. *Protoplasma* **227**: 25–36
- Johnson MA, Preuss D** (2002) Plotting a course: multiple signals guide pollen tubes to their targets. *Dev Cell* **2**: 273–281
- Ketelaar T, Anthony RG, Hussey PJ** (2004) Green fluorescent protein-mTalin causes defects in actin organization and cell expansion in *Arabidopsis* and inhibits actin depolymerizing factor's actin depolymerizing activity *in vitro*. *Plant Physiol* **136**: 3990–3998
- Kost B, Lemichez E, Spielhofer P, Hong Y, Tolia K, Carpenter C, Chua NH** (1999) Rac homologues and compartmentalized phosphatidylinositol 4, 5-bisphosphate act in a common pathway to regulate polar pollen tube growth. *J Cell Biol* **145**: 317–330
- Krinke O, Ruelland E, Valentova O, Vergnolle C, Renou JP, Taconnat L, Flemer M, Burketova L, Zachowski A** (2007) Phosphatidylinositol 4-kinase activation is an early response to salicylic acid in *Arabidopsis* suspension cells. *Plant Physiol* **144**: 1347–1359
- Lavy M, Bloch D, Hazak O, Gutman I, Poraty L, Sorek N, Sternberg H, Yalovsky S** (2007) A novel ROP/RAC effector links cell polarity, root-meristem maintenance, and vesicle trafficking. *Curr Biol* **17**: 947–952
- Lee YJ, Szumlanski A, Nielsen E, Yang Z** (2008) Rho-GTPase-dependent filamentous actin dynamics coordinate vesicle targeting and exocytosis during tip growth. *J Cell Biol* **181**: 1155–1168
- Lind J, Bönig I, Clarke A, Anderson M** (1996) A style-specific 120-kDa glycoprotein enters pollen tubes of *Nicotiana glauca* *in vivo*. *Sex Plant Reprod* **9**: 75–86
- Lovy-Wheeler A, Cardenas L, Kunkel J, Hepler P** (2007) Differential organelle movement on the actin cytoskeleton in lily pollen tubes. *Cell Motil Cytoskeleton* **64**: 217–232
- Moscattelli A, Ciampolini F, Rodighiero S, Onelli E, Cresti M, Santo N, Idilli A** (2007) Distinct endocytic pathways identified in tobacco pollen tubes using charged nanogold. *J Cell Sci* **120**: 3804–3819
- Nebenfuhr A, Ritzenthaler C, Robinson DG** (2002) Brefeldin A: deciphering an enigmatic inhibitor of secretion. *Plant Physiol* **130**: 1102–1108

- Parton RM, Fischer-Parton S, Trewavas AJ, Watahiki MK** (2003) Pollen tubes exhibit regular periodic membrane trafficking events in the absence of apical extension. *J Cell Sci* **116**: 2707–2719
- Parton RM, Fischer-Parton S, Watahiki MK, Trewavas AJ** (2001) Dynamics of the apical vesicle accumulation and the rate of growth are related in individual pollen tubes. *J Cell Sci* **114**: 2685–2695
- Preuss ML, Serna J, Falbel TG, Bednarek SY, Nielsen E** (2004) The *Arabidopsis* Rab GTPase RabA4b localizes to the tips of growing root hair cells. *Plant Cell* **16**: 1589–1603
- Samaj J, Müller J, Beck M, Böhm N, Menzel D** (2006) Vesicular trafficking, cytoskeleton and signalling in root hairs and pollen tubes. *Trends Plant Sci* **11**: 594–600
- Staiger CJ, Yuan M, Valenta R, Shaw PJ, Warn RM, Lloyd CW** (1994) Microinjected profilin affects cytoplasmic streaming in plant cells by rapidly depolymerizing actin microfilaments. *Curr Biol* **4**: 215–219
- Tse YC, Mo B, Hillmer S, Zhao M, Lo SW, Robinson DG, Jiang L** (2004) Identification of multivesicular bodies as prevacuolar compartments in *Nicotiana tabacum* BY-2 cells. *Plant Cell* **16**: 672–693
- Ueda T, Uemura T, Sato MH, Nakano A** (2004) Functional differentiation of endosomes in *Arabidopsis* cells. *Plant J* **40**: 783–789
- Ueda T, Yamaguchi M, Uchimiya H, Nakano A** (2001) Ara6, a plant-unique novel type Rab GTPase, functions in the endocytic pathway of *Arabidopsis thaliana*. *EMBO J* **20**: 4730–4741
- van Leeuwen W, Okresz L, Bogre L, Munnik T** (2004) Learning the lipid language of plant signalling. *Trends Plant Sci* **9**: 378–384
- Vermeer J, Thole J, Goedhart J, Nielsen E, Munnik T, Gadella TJ** (2009) Imaging phosphatidylinositol 4-phosphate dynamics in living plant cells. *Plant J* **57**: 356–372
- Vidali L, McKenna ST, Hepler PK** (2001) Actin polymerization is essential for pollen tube growth. *Mol Biol Cell* **12**: 2534–2545
- Wang Q, Kong L, Hao H, Wang X, Lin J, Samaj J, Baluska F** (2005) Effects of Brefeldin A on pollen germination and tube growth: antagonistic effects on endocytosis and secretion. *Plant Physiol* **139**: 1692–1703
- Wilsen K, Lovy-Wheeler A, Voigt B, Menzel D, Kunkel J, Hepler P** (2006) Imaging the actin cytoskeleton in growing pollen tubes. *Sex Plant Reprod* **19**: 51–62
- Wu G, Gu Y, Li S, Yang Z** (2001) A genome-wide analysis of *Arabidopsis* Rop-interactive CRIB motif-containing proteins that act as Rop GTPase targets. *Plant Cell* **13**: 2841–2856
- Zhang Y, He J, McCormick S** (2009) Two *Arabidopsis* AGC kinases are critical for the polarized growth of pollen tubes. *Plant J* **58**: 474–484
- Zhang Y, McCormick S** (2007) A distinct mechanism regulating a pollen-specific guanine nucleotide exchange factor for the small GTPase Rop in *Arabidopsis thaliana*. *Proc Natl Acad Sci USA* **104**: 18830–18835
- Zonia L, Munnik T** (2009) Uncovering hidden treasures in pollen tube growth mechanics. *Trends Plant Sci* **14**: 318–327

Supplemental Figure 1. Fluorescent protein probes expressed in tobacco pollen.

(A) A pollen tube expressing YFP-RabA4b that labels transport vesicles. Inset shows a longitudinal tail of RabA4b labeling in a transformed pollen tube.

(B) A pollen tube expressing ARA6-YFP that labels endosomes.

(C) A pollen tube expressing YFP-ARA7 that labels endosomes.

(D) A pollen tube expressing YFP-mTalin that labels the actin cytoskeleton.

Left panels, YFP channel; right panels, transmitted light.

Scale bars = 20 μ m.

Supplemental Figure 2. Pollen tube morphology and growth rate were not affected in pollen expressing fluorescent probes.

(A) Pollen tube width.

(B) Pollen tube growth rate.

Supplemental Figure 3. Effect of BFA treatment on transport vesicles labeled by YFP-RabA4b and FM4-64. Pollen tubes expressing YFP-RabA4b treated with BFA at 15 min (A), 30 min (B) and 45 min (C). 5 min before imaging, 4 mM FM4-64 in DMSO was added to the medium. Top images were taken with the YFP channel, middle images were taken with the RFP channel. Merged images are shown at the bottom. Scale bar = 20 μ m.

Supplemental Figure 4. Effect of Wortmannin treatment on transport vesicles labeled by YFP-RabA4b and FM4-64.

Pollen tubes expressing YFP-RabA4b treated with Wortmannin at 30 min (A), 60 min (B) and 90 min (C). 5 min before imaging, 4 mM FM4-64 in DMSO was added to the medium. Top images were taken with the YFP channel, middle images were taken with the RFP channel. Merged images are shown at the bottom. Scale bar = 20 μ m.

Supplemental Figure 5. Effect of BFA treatment on pollen tubes expressing either ARA6-YFP (A) or YFP-ARA7 (B) and labeled with FM4-64. Top images were taken with the YFP channel and bottom images were taken with the RFP channel. Scale bar = 20 μ m.

Supplemental Figure 6. Effect of Wortmannin treatment on pollen tubes expressing either ARA6-YFP (A) or YFP-ARA7 (B) and labeled with FM4-64. Top images were taken with the YFP channel and bottom images were taken with the RFP channel. Scale bar = 20 μ m.

Supplemental Figure 7. Effects of BFA and Wortmannin treatments on pollen tubes co-expressing ARA6-CFP and YFP-ARA7. Top images were taken with the CFP channel; middle images with the YFP channel. Merged images are shown at the bottom. Scale bar = 20 μ m.

Supplemental Figure 8. The effects of actin disrupting drugs on the YFP-mTalin labeling pattern.

(A) A pollen tube treated with LatB for 30 min. Arrow indicates where the F-actin ring would be localized in non-treated tubes.

(B) A pollen tube treated with LatB for 60 min. Arrow indicates where the F-actin ring would be localized in non-treated tubes.

(C) A pollen tube treated with Jas for 10 min. Note that a few actin cables remained intact (shown with asterisk), while thick actin patches were already formed.

(D) A tube treated with Jas for 40 min. No actin cables were visible, and instead, thick actin patches were present throughout the tube.

Dotted lines show the contour of the apex of pollen tubes. Scale bar = 20 μ m.

Supplemental Movie 1. Transport vesicles labeled by YFP-RabA4b in a growing control tube.

Supplemental Movie 2. Transport vesicles labeled by YFP-RabA4b in a pollen tube treated with BFA for 30 min.

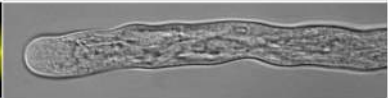
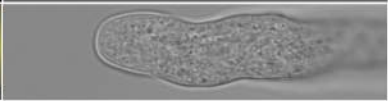
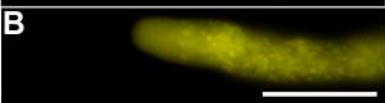
Supplemental Movie 3. Transport vesicles labeled by YFP-RabA4b in a pollen tube treated with Wortmannin for 30 min.

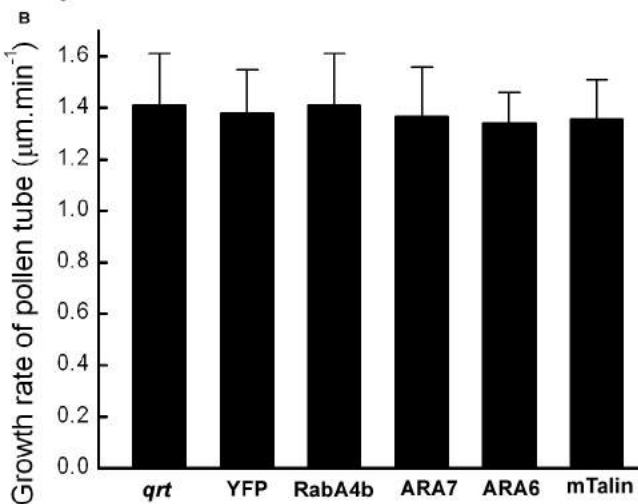
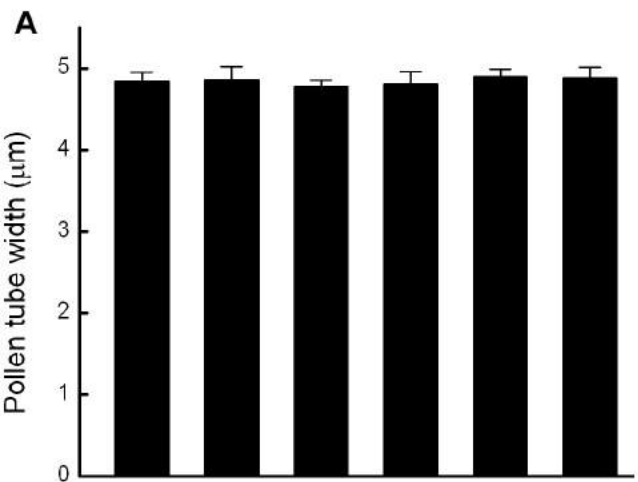
Supplemental Movie 4. ARA7-positive endosomes treated with Wortmannin for 60 min.

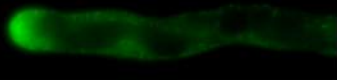
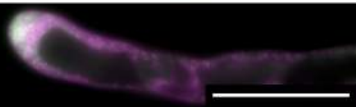
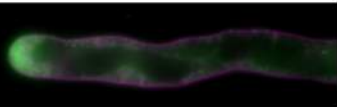
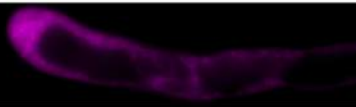
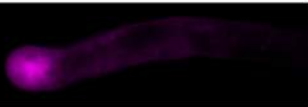
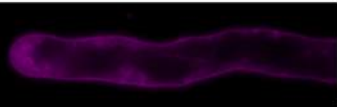
Supplemental Movie 5. ARA6-positive endosomes treated with BFA for 45 min.

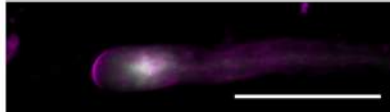
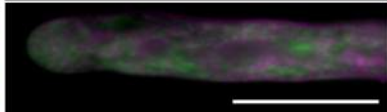
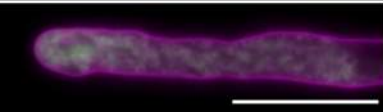
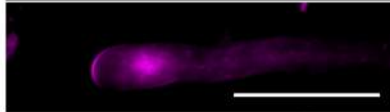
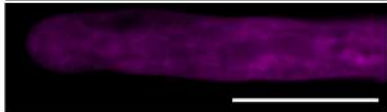
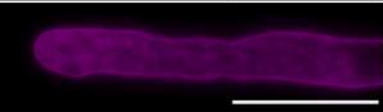
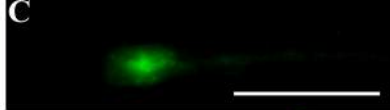
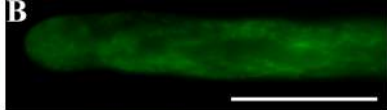
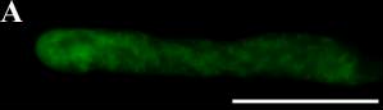
Supplemental Movie 6. Transport vesicles labeled by YFP-RabA4b in a pollen tube treated with LatB for 20 min.

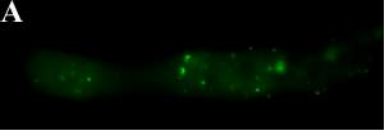
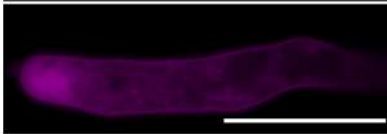
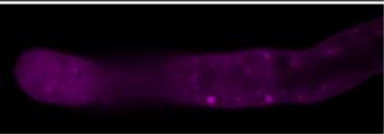
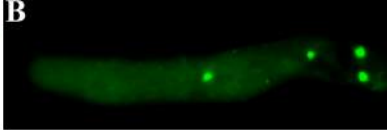
All movies are 30 frames taken at 30 sec intervals and play at 5 frames/sec.

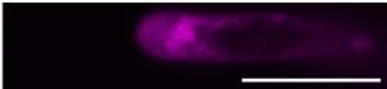
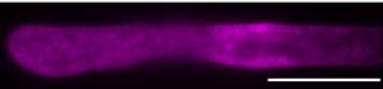
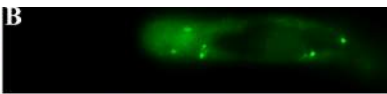
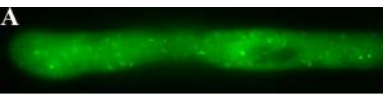


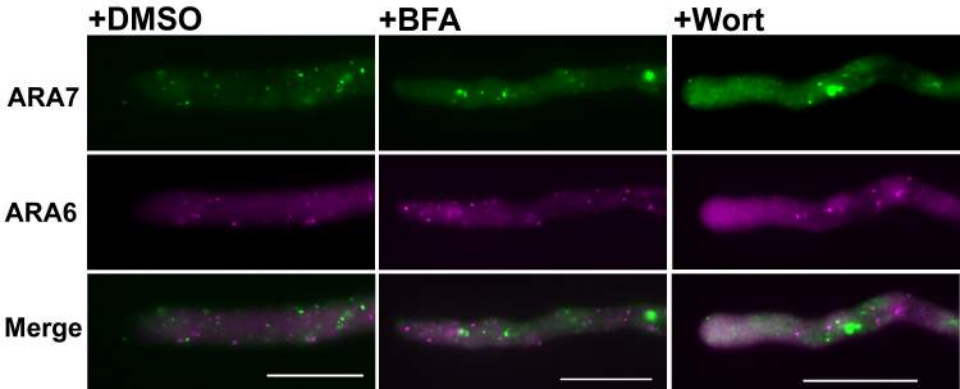


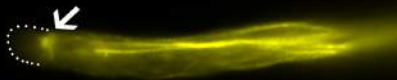
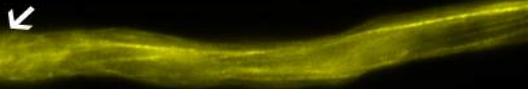
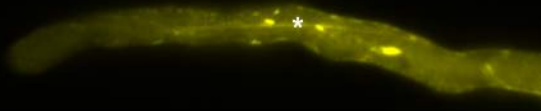
A**B****C**



A**B**





A**B****C****D**